Effect of Mixer Resident Time on the Overall Moduli of Polymer Blends

ZHIMIN XIE,[1,2] DINGHAO ZHANG,[1] JING SHENG,[1] KAIXU SONG[3]

[1] School of Materials Science and Engineering, Tianjin University, Tianjin 300072, P.R. China

[2] The State Key Laboratory of Polymer Materials Engineering, Sichuan University, Chengdu 610065, P.R.China

[3] Department of Chemical Engineering, Tianjin University, Tianjin 300072, P.R.China

Received 1 June 2001; revised 24 September 2001

ABSTRACT: The overall moduli tensor of polymer blends is one of the most important characteristics of microscopic morphology development. This article focused on the analysis of dependence of the moduli on mixer resident time in terms of polypropylene–polystyrene (PP/PS) and polypropylene–polyamide1010 (PP/PA1010) blends. Tensile tests on the PP/PS and PP/PA1010 blends with a series of mixer resident times showed a marked change during the initial mixing stage, which may be due to the evolution of particle size and distribution from inhomogeneous to homogeneous. The two cases of periodic spatial distribution of the identical spherical particles were proposed to model the well-dispersed and slightly aggregating morphologies in the steady state. Based on the micromechanical model, the moduli of polymer blends were calculated by incorporating the influences of spatial distribution and Poisson's ratio of dispersed particles. Theoretical results indicated that spatial distribution should have little effect on the overall moduli in the steady state. Analysis of the blend system PP/PA1010 with and without compatibilizing agent showed good agreement between the calculations and experiments. Because the interfacial properties were not taken into account, the model gave an overestimate prediction for immiscible blends, like PP/PS for example. © 2002 Wiley Periodicals, Inc. J Appl Polym Sci 85: 307–314, 2002

Key words: blends; microstructure; modeling; modulus

INTRODUCTION

Polymer blends are macroscopically homogeneous although heterogeneous on a microscopic scale. The macroscopic properties of the blends are strongly dependent on the component properties, composition, and morphology; that is, the size, shape, and distribution of the components. Many papers are dedicated to the relationship between morphology and mechanical properties experimentally and theoretically. Van Gheluwe et al.,[1] for instance, discussed the effect of different morphologies, such as fiber- and rod-like dispersed phases, on the mechanical properties. Willemse et al.[2] studied the tensile moduli of co-continuous polymer blends polyethylene–polypropylene (PE/PP) and polyethylene–polystyrene (PE/PS). Veenstra et al.[3] made a comparison investigation into the mechanical properties of co-continuous polymer blends with the properties of the same polymers blends with a drop/matrix morphology. Kunori and Geil[4,5] investigated the morphology–

Correspondence to: J. Sheng (shengxu@public.tpt.tj.cn)
Contract Grant Sponsor: National Natural Science Foundation, China; contract grant number 59733070).

Journal of Applied Polymer Science, Vol. 85, 307–314 (2002)

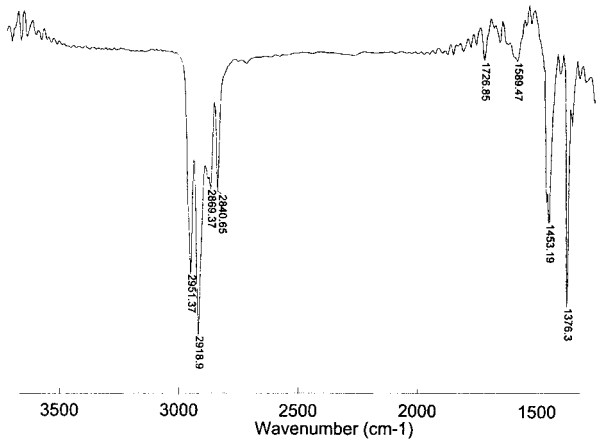

Figure 1 FTIR spectrum of PP/g-MAH.

property relationships in detail and evaluated the applicability of composites' models to the polycarbonate-based blends. Much less theoretical analysis, however, was concerned with the influences of the spatial distribution and Poisson's ratio of the dispersed particle. It is well known that blend morphology is determined by the processing conditions, concentration, and rheological parameters of the components.[6,7] Blend morphology formation is a result of competition between deformation, breakup, and coalescence of melt polymer drops in the processing flow field. As for the spherical morphology composed of a droplet of the minor component dispersed in the major component in a low concentration system, the particle size and distribution tend to be steady-state from inhomogeneous with increasing mixer resident time, which should be reflected by the macroscopic mechanical properties. The overall moduli tensor of blends is one of the most important characteristics of the microscopic morphology development. A number of composites theories have been proposed to predict the modulus of composite system. The self-consistent method, one of the most powerful methods to solve the many-particle problem, enables one to obtain good approximations in many important cases,[8] but the size and interaction of inclusions are discarded. Du and Wu[9,10] took these factors into account and introduced the integral method of the related function to give a satisfactory prediction of the effective elastic moduli of fiber-reinforced epoxy resin in particular. In this article we discuss the dependence of the moduli on the morphology formation in terms of polypropylene–polystyrene (PP/PS) and polypropylene–polyamide 1010 (PP/PA) blends by using the micromechanical model.

THEORETICAL

Micromechanical Model

Following the method of the effective field,[8] the stress and strain in the inhomogeneous medium can be expressed by

$$\varepsilon(x) = \varepsilon_0(x) - \sum_{i=1}^{n} \int_V K_0(x - x')C_{1i}\varepsilon_i^+(x')V_i(x')\,dx' \tag{1}$$

$$\sigma(x) = \sigma_0(x) - \sum_{i=1}^{n} \int_V \times S_0(x - x')B_{1i}\sigma^+(x')V_i(x')\,dx' \tag{2}$$

where n is the number of the inclusions, ε_0 and σ_0 are the external strain and stress fields, respectively, $\varepsilon_i^+(x)$ and $\sigma_i^+(x)$ are the fields of strain and stress inside the ith inclusion, respectively, $V_i(x)$ is the characteristic function of the region occupied by the ith inclusion, C_{1i} is the elastic moduli difference between the ith inclusion and matrix, B_{1i} is the elastic compliance difference, and K_0 and S_0 are the Green's operators corresponding to stress and strain, respectively.

The effective elastic moduli tensor is defined as

$$C^* = \frac{\langle\sigma(x)\rangle}{\langle\varepsilon(x)\rangle} \tag{3}$$

Table I Mechanical Properties of the Pure Polymers

Method	PS	PP (grade A)	PP (grade B)	PA1010
Young's modulus (MPa)	2985	945	1765	1427
Poisson's ratio	0.27	0.21	0.21	0.23

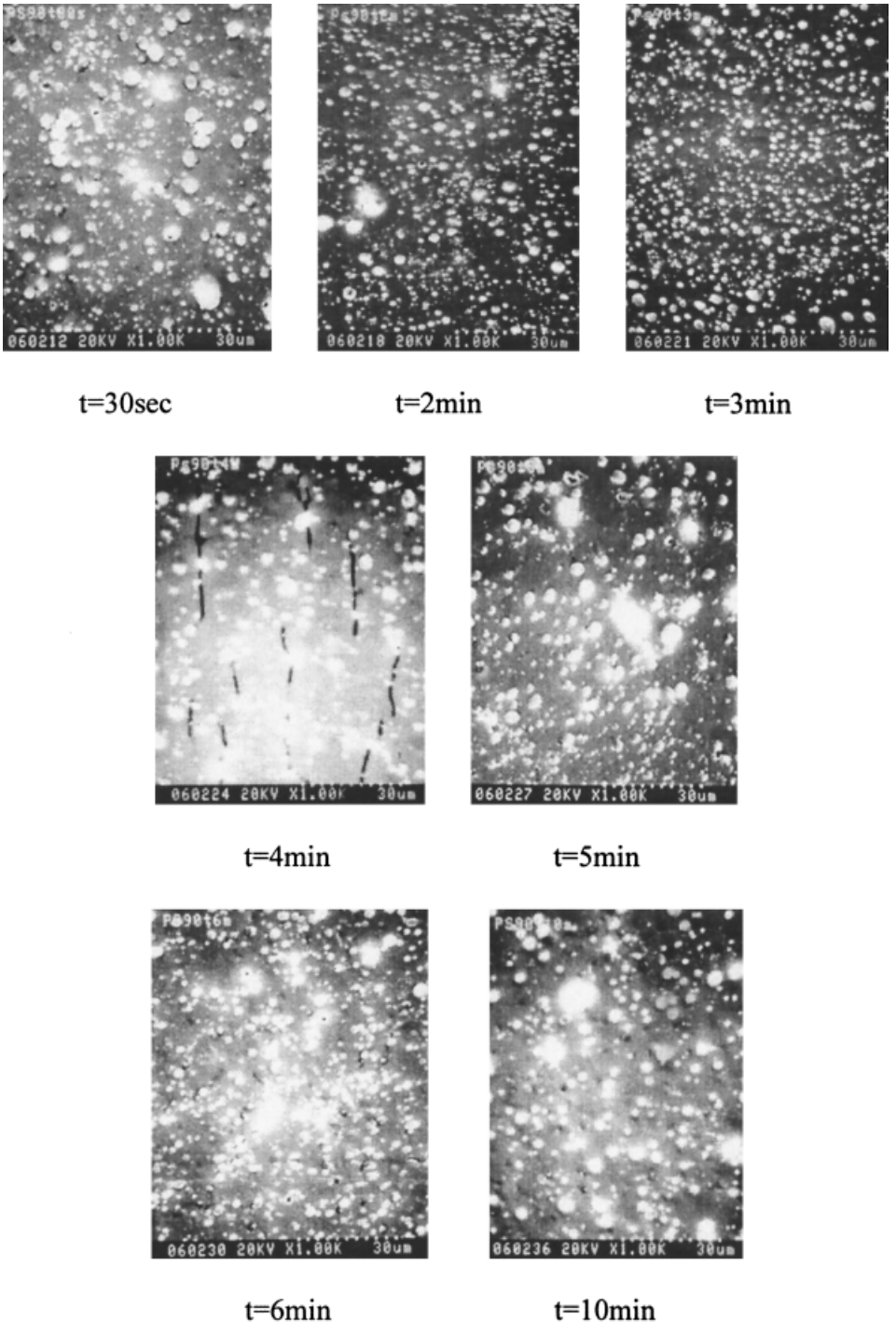

Figure 2 SEM photographs of the PP/PS (10/90) blends with different mixer resident times.

with

$$\langle f(x) \rangle = \frac{1}{V} \int_V f(x)\, \mathrm{d}x \qquad (4)$$

where V is the volume of inhomogeneous medium. In the case of a homogeneous medium containing identical spherical inclusions (i.e., $C_{1i} = C_1 = \text{constant}$ and $V_i = V_f = \text{constant}$), the finial explicit expression for the elastic mod-

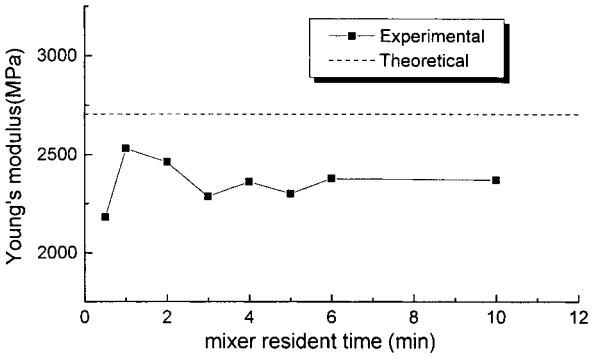

Figure 3 Young's modulus of the PP/PS1010 blend with different mixer resident times.

uli tensor is deduced by Du and Wu[9,10] as follows:

$$C^* = C_0 + V_f C_1 \Bigg[I + (1 - V_f) A_0 C_1 + T^{-1} \Bigg(\sum_{i=1, i \neq j}^{n} G_{ij} \Bigg) T C_1 \Bigg]^{-1} \quad (5)$$

in which C_0 and C_1 are the elastic moduli of medium and inclusion, respectively, V_f is the volume percentage of the inclusions, I is the unit tensor of fourth order, A_0 is the Eshelby tensor related to the Lame's constants of the medium, and T is the linear transformation matrix for the strain tensor (see ref.10). It should be noted that the last term in the bracket (see Appendix) reflects the microstructure characteristics to some degree; that is, the shape, size, distribution, and interaction of the inclusions. In other words, if the size and spatial distribution of the inclusions and the component properties, such as elastic moduli and Poisson's ratio, are given, then the overall elastic moduli should be obtained by using eq. 5.

EXPERIMENTAL

PS with molecular weights of $M_w = 5.8 \times 10^5$ and $M_w = 2.7 \times 10^5$, density of 1.05g/cm^3, and glass transition temperature of 111°C (Dynamic Mechanical Analysis), and PP with glass transition temperature of 17°C (two grades) from Beijing Yanshan Petrochemical Company (Beijing, China) were used. PS and PP (grade A) were dried at 80°C for 4 h and blended in a mixing apparatus (Model XXS-30, Mixer with screw diameter 35 mm, China) at 30 rpm and 220°C. PA1010 from Tianjin Zhonghe Chemical Plant (Tianjin, China) and PP (grade B) with and/or without compatibilizing agent polypropylene–graft-maleic anhydride(PP/g-MAH) dried before compounding individually were melt blended at 200°C. The Fourier transform infrared (FTIR) spectra of the PP/g-MAH is shown in Figure 1. The absorption band observed at 1727 cm^{-1} can be assigned to the absorption of the carbonyl groups (—C═O) of cyclic anhydride. The polymer blends were mould compressed in a common heating press at ~ 20 MPa and 180°C for 1 min and then cooled under pressure 20 MPa with a resident time of 5 min at room temperature. The plates were punched to several dumb-bell shape specimens for mechanical test. Pieces of the PP/PS blend plate were broken in liquid nitrogen, and the fracture surfaces were etched with acetone with a resident time of 1 min. They were then coated with Au-Pd for observation in a scanning electron microscope (SEM; Hitachi X-650, Japan). Pieces of the PP/PA1010 blend plate were broken in liquid nitrogen for morphology observation with a Philips XL30 SEM. The modulus and Poisson's ratio were obtained from the tensile tests conducted with an Instron Tester (model 1186) at a cross-head speed of 5 mm/min and ambient temperature of 25°C. The mechanical properties of the pure polymers measured are listed in Table I.

RESULTS AND DISCUSSION

A series of morphologies of a PP(grade A)/PS (10/90) blend with different mixer resident times is shown in Figure 2. As expected, the particle size

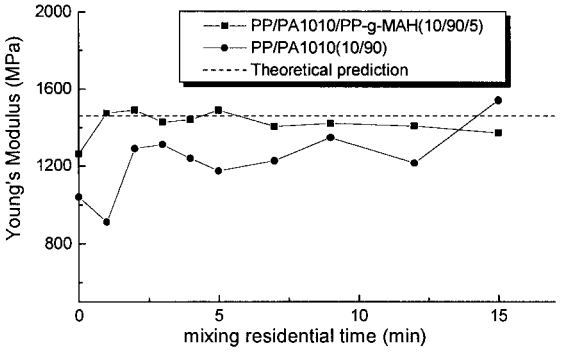

Figure 4 Young's modulus of the PP/Pa (10/90) blend with different mixer resident times.

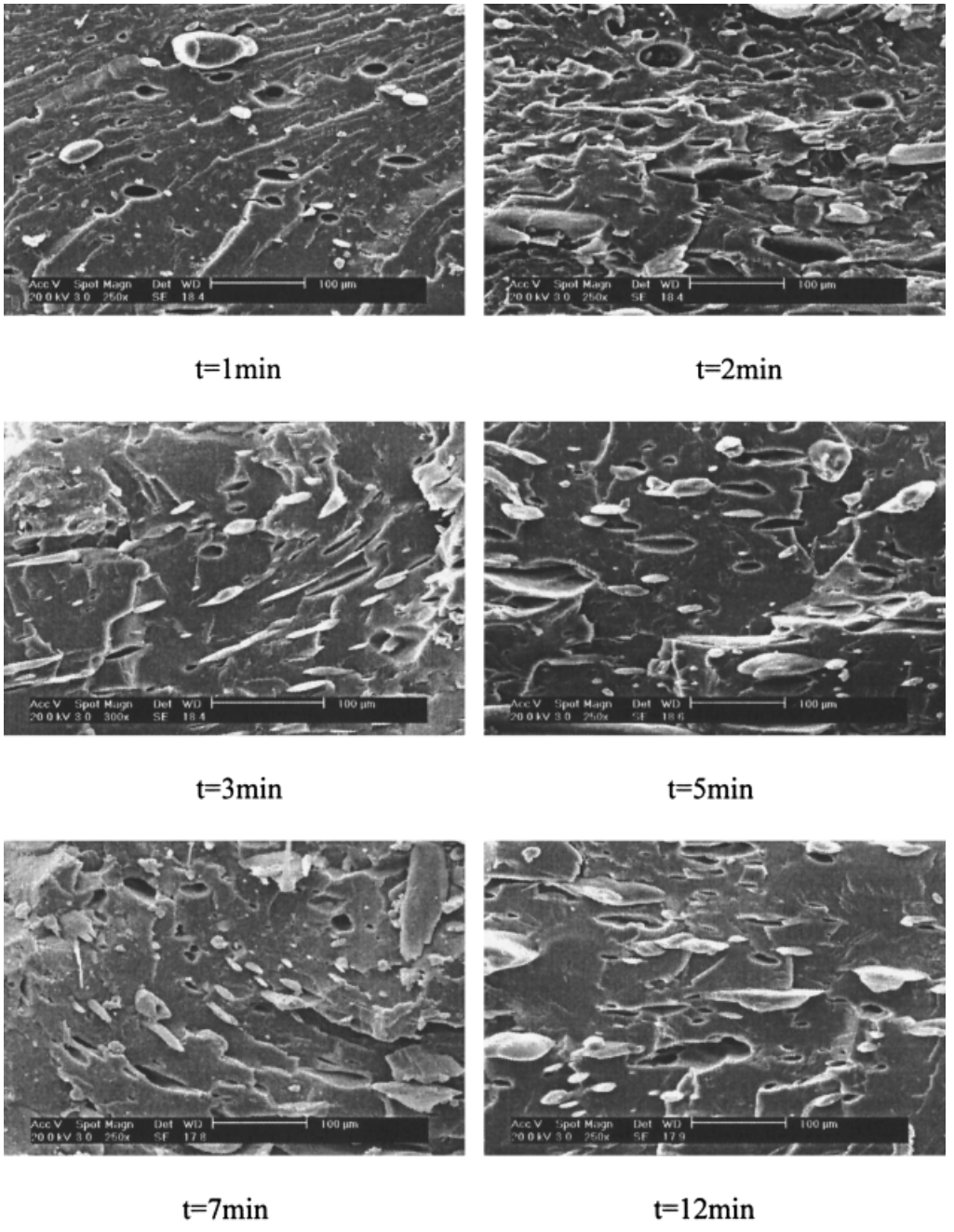

Figure 5 SEM photographs of the PP/PA1010 (10/90) blend with different mixer resident times.

initially decreased before 3 min, indicating the predominance of the breakup of polymer drops. After that point, with increase of coalescence arising from forced collision of the dispersed particles during the mixing processing, the particle size increased and the particles reaggregation produced a mixture of sizes. The dynamic equilibrium of the breakup and coalescence leaded finally to a relative steady-state particle size and distribution. The morphology development should also be reflected by the overall elastic modulus. The marked change in the modulus before 3 min, which may be due to the evolution of particle size and distribution from inhomogeneous to homogeneous, is shown in Figure 3. Because the morphology developed and tended to a steady state, the

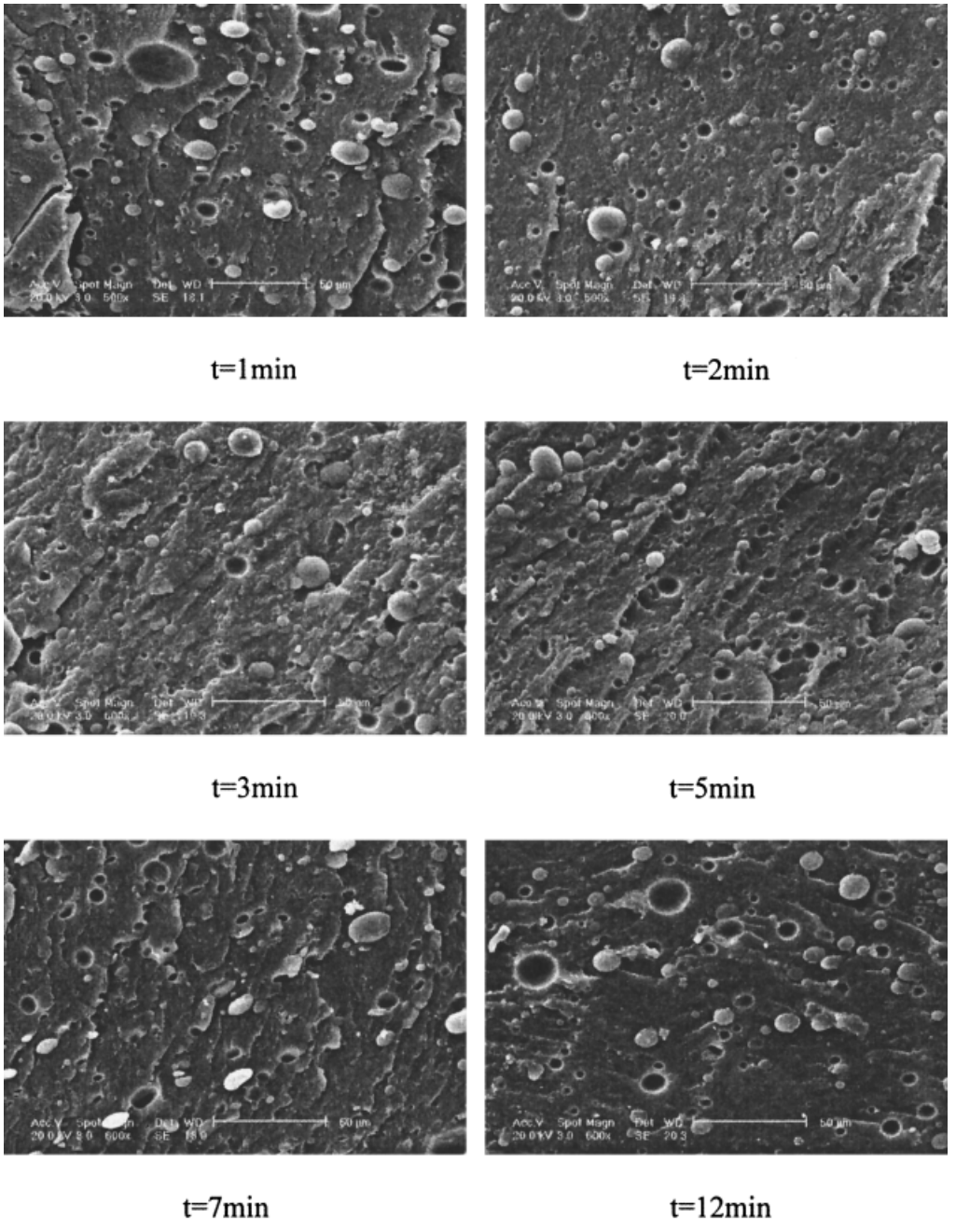

Figure 6 SEM photographs of the PP/PS1010/PP-g-MAH (10/90/5) blends with different mixer resident times.

Young's modulus had a little change. Tensile tests on the blends PP(grade B)/PA1010 (10/90) showed the same trend, as shown in Figure 4. A series of SEM photographs of PP/PA1010 blend with and/or without-MAH are shown in Figures 5 and 6, respectively. There is little change in morphology after 3 min of mixing, and the morphology of PP/PA1010/PP–g-MAH (10/90/5) consists of spherical or ellipsoid particles in a matrix in which the PA1010 is the dispersed phase.

Consider two cases of periodic spatial distribution of the identical spherical particles, cubic arrangement (case 1) and body arrangement (case 2), to model the well-dispersed and slightly aggregating morphologies in the steady state, respectively. The two representative elements are shown in

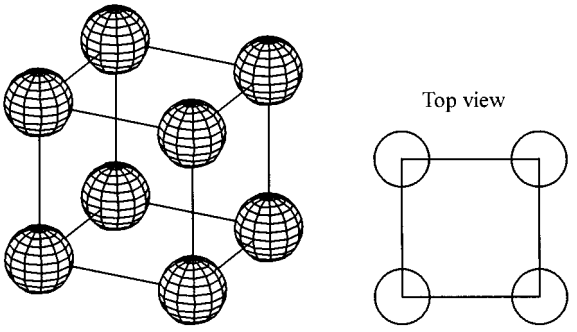

Figure 7 An element for cubic arrangement.

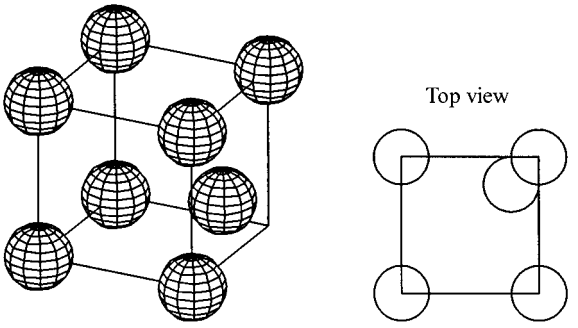

Figure 8 A 1/8 element for the body arrangement.

Figures 7 and 8. Although the unreachable condition limits case 2 to a valid range of $< 30\%$ volume of dispersed phase, it is sufficient to describe the drop/matrix morphology, because the co-continuous morphology will be formed around the high volume fraction corresponding to phase inversion. By applying the integral method of the related function (eq. 5), the moduli of the blends were calculated as 2706.74 and 2706.73 MPa for cases 1 and 2, respectively. No difference indicated that the spatial distribution of dispersed phase should have little effect on the overall moduli of the blends when the drop/matrix morphology gets to the steady state, which is the same conclusion as with the experiments on blends PP/PS, PP/PA1010, and PP/PA1010/PP–g-MAH. In addition, an important assumption of the perfect bond between phases implied in the theory might not be appropriate for immiscible blends, so a discrepancy between the theoretical and experimental was found in the PP/PS as well as PP/PA1010(10/90) blends, as shown in Figures 3 and 4. Because the addition of compatibilizing agent-MAH improves the interfacial adhesion, the theoretical prediction (1457 MPa) is close to the experimental results. It is anticipated that one may achieve the theoretical moduli for the blends PP/PS by improving the interfacial properties. Similar conclusions about the influence of the interface on the mechanical properties were also drawn by Kunori and Geil[4, 5] based on the comparison investigation on polycarbonate-based blends.

CONCLUSIONS

Tensile tests on the PP/PS and PP/PA1010 blends with a series of mixer resident times showed a marked change in moduli during the initial mixing stage, which may be due to the evolution of particle size and distribution from inhomogeneous to homogeneous. The two cases of periodic spatial distribution of the identical spherical particles were proposed to model the well-dispersed and slightly aggregating morphologies in the steady state. Based on the micromechanical model, the moduli of polymer blends were calculated. Theoretical analysis indicated that spatial distribution of dispersed phase should have little effect on the overall moduli in the steady state. Analysis of the blend system PP/PA1010 with and/or without compatibilizing agent showed good agreement between the calculations and experiments. Because the interfacial properties were not taken into account in the analysis, the model gave an overestimate prediction for immiscible blends like PP/PS.

APPENDIX

A detailed description for the tensor G_{ij} can be written as follows:[10]

$$(G_{ij})_{1111} = \frac{1}{8\mu(\lambda + 2\mu)} \int_0^{0_{ij}} \left[2(\mu - \lambda) + 6(2\lambda + \mu)\sin^2\theta - \frac{45}{4}(\lambda + \mu)\sin^4\theta \right] \sin\theta f_{ij}(\theta)\, d\theta \quad \text{(A1)}$$

$$(G_{ij})_{3333} = \frac{1}{4\mu(\lambda + 2\mu)} \int_0^{0_{ij}} [\mu - \lambda + 6(2\lambda + \mu)\cos^2\theta - 15(\lambda + \mu)\cos^4\theta]\sin\theta f_{ij}(\theta)\, d\theta \quad \text{(A2)}$$

$$(G_{ij})_{1122} = \frac{\lambda + \mu}{8\mu(\lambda + 2\mu)} \int_0^{0_{ij}} \left[-2 + 6\sin^2\theta - \frac{15}{4}\sin^4\theta \right] \sin\theta f_{ij}(\theta)\, d\theta \tag{A3}$$

$$(G_{ij})_{1133} = \frac{\lambda + \mu}{8\mu(\lambda + 2\mu)} \int_0^{0_{ij}} [1 + 3\cos^2\theta - 15\sin^2\theta\cos^2\theta] \sin\theta f_{ij}(\theta)\, d\theta \tag{A4}$$

$$(G_{ij})_{1212} = \frac{1}{32\mu(\lambda + 2\mu)} \int_0^{0_{ij}} [8\mu + 12\lambda\sin^2\theta - 15(\lambda + \mu)\sin^4\theta] \sin\theta f_{ij}(\theta)\, d\theta \tag{A5}$$

$$(G_{ij})_{3131} = \frac{1}{16\mu(\lambda + 2\mu)} \int_0^{0_{ij}} [3\lambda + 4\mu + 3\lambda\cos^2\theta - 30(\lambda + \mu)\sin^2\theta\cos^2\theta] \sin\theta f_{ij}(\theta)\, d\theta \tag{A6}$$

with

$$f_{ij}(\theta) = 2\ln\left[\frac{d_{ij}}{2r}\cos\theta + g_{ij}(\theta)\right] - \ln\left[\left(\frac{d_{ij}}{2r}\right)^2 - 1\right] - \frac{1}{2}\left(\frac{d_{ij}}{2r}\right)\cos\theta g_{ij}(\theta) + \left[\frac{3d_{ij}}{4r} - \frac{1}{2}\left(\frac{d_{ij}}{2r}\right)^3\left(\frac{\sin\theta^2}{2} + 1\right)\right]\cos\theta\ln\frac{1 + g_{ij}(\theta)}{1 - g_{ij}(\theta)} + \left[\frac{3d_{ij}}{4r} - \frac{1}{2}\left(\frac{d_{ij}}{2r}\right)^3\right]\ln\frac{\cos\theta - g_{ij}(\theta)}{\cos\theta + g_{ij}(\theta)} \tag{A7}$$

$$g_{ij}(\theta) = \left[1 - \left(\frac{d_{ij}}{2r}\right)^2\sin^2\theta\right]^{1/2} \tag{A8}$$

$$\theta_{ij} = \sin^{-1}\frac{2r}{d_{ij}} \tag{A9}$$

where λ and μ denote the Lame's constants of inclusion, r is the sphere radius, and d_{ij} is the distance between the spheres i and j, and other components of G_{ij} are zeros.

REFERENCES

1. Van Gheluwe, P.; Favis, B.D.; Chalifoux, J.-P. J Mater Sci 1988, 23, 3910–3920.
2. Willemse, R.C.; Speijer, A.; Langeraar, A.E.; Posthuma de Boer, A. Polymer 1999, 40, 6645–6650.
3. Veenstra, H.; Verkooijen, P.C.J.; Van Lent, B.J.J.; Van Dam, J.; De Boer, A.P.; Nijhof, A.P.H.J. Polymer 2000, 4, 1817–1826.
4. Kunori, T.; Geil, P.H. J Macromol Sci-Phys B 1980, 18(1), 93–134.
5. Kunori, T.; Geil, P.H. J Macromol Sci-Phys B18 1980, (1),35–175.
6. Utracki, L.A.; Shi, Z.H. Polym Eng Sci 1992, 32(24),1824–1833.
7. Lee, H.M.; Park, O.O. J Rheol 1994, 38(5), 1405–1425.
8. Kunin, I.A. Elastic media with microstructure II; Heidelberg, Germany: Springer-Verlag, 1983.
9. Du, S.; Wu, L. Acta Mater Compos Sin 1994, 11(1),105–111.
10. Wu, L. Meso-theory on the elastic media with inclusions and distributed cracks. Ph.D. Thesis, Harbin Institute of Technology, 1992.